International Journal of General Medicine

Dovepress
open access to scientific and medical research

Open Access Full Text Article

ORIGINAL RESEARCH

BCL9 is a Risk Factor of Neck Lymph Nodes Metastasis and Correlated with Immune Cell Infiltration in Papillary Thyroid Carcinoma

Rui Zhang[1,*], Zhengwei Gui[2,*], Jianguo Zhao[1], Lu Zhao[2]

[1]Department of Thyroid and Breast Surgery, Wuhan No. 1 Hospital, Wuhan, 430030, People's Republic of China; [2]Department of Thyroid and Breast Surgery, Tongji Hospital Affiliated with Tongji Medical College of Huazhong University of Science and Technology, Wuhan, 430030, People's Republic of China

*These authors contributed equally to this work

Correspondence: Lu Zhao, Department of Thyroid and Breast Surgery, Tongji Hospital affiliated with Tongji Medical College of Huazhong University of Science and Technology, No. 1095 of Jiefang Avenue, Wuhan, 430030, People's Republic of China, Email luzhao268@outlook.com

Purpose: B-cell lymphoma 9 (BCL9), a key transcription co-activator of the Wnt pathway, contributed to tumor progression and metastasis in various tumors, whereas, the role of BCL9 in papillary thyroid cancer (PTC) has not been investigated.

Methods: We acquired PTC gene expression data from The Cancer Genome Atlas (TCGA) database. Fifty-nine PTC tissues were applied to validate the clinical significance of BCL9. Cell experiments were applied to investigate the role of BCL9. Bioinformatics analysis was employed to investigate the biological functions of BCL9.

Results: We found that BCL9 was higher expressed ($P < 0.05$) and an independent risk factor for lymph node metastasis ($OR = 3.770$, $P = 0.025$), as well as associated with poorer progression-free survival (PFS) ($P = 0.049$) in PTC. BCL9 knockdown inhibited proliferation and invasion of PTC cells. BCL9 was positively associated with the key genes of Wnt/β-catenin and MAPK pathway by co-expression analysis. GO, KEGG and GSEA analysis showed BCL9 might participated in PPAR, cAMP, and focal adhesion pathway. CIBERSORT analysis found BCL9 was negatively associated with CD8+ T cells and NK cell infiltration and positively with PD-L1 expression.

Conclusion: Therefore, BCL9 was associated with lymph node metastasis and shorter PFS of PTC, due to promotion of PTC cell proliferation and invasion, activation of Wnt/β-catenin and MAPK pathway, inhibition of CD8+ T and NK cell infiltration, and promotion of PD-L1 expression.

Keywords: BCL9, papillary thyroid cancer, lymph node metastasis, tumor immune microenvironment, tumor-infiltrating immune cells

Introduction

Thyroid cancer (TC) is the endocrine malignant tumor with the highest incidence rate. Eighty-five percent of all thyroid cancer subtypes are papillary thyroid cancer (PTC), with a growing incidence rate every year, especially in developed countries.[1] Due to the widely applied ultrasonography in the early diagnosis of TC, most patients with PTC have a relatively satisfactory clinical prognosis followed the standard surgery therapy and thyroid stimulating hormone (TSH) inhibition or radioactive iodine.[2] However, nearly 50% PTC patients still face a presence of an approximately 30% recurrence rate and 8.6% mortality for a three-decade period,[3] and either thyroid ultrasonography or FNAC sometimes provides indeterminate reports which cause difficulties in interpretation and clinical management.[4] Therefore, it is extraordinarily significant to uncover promising prognostic markers for PTC patients to early screening, timely treatment, effective monitoring and prolonged survival time.

Wnt/β-catenin pathway is involved in many key aspects of cancer development,[5] including in thyroid carcinoma.[6,7] The progression and metastatic activities of PTC have been verified to be correlated with the downregulation of

Received: 23 January 2024
Accepted: 4 April 2024
Published: 16 April 2024

E-cadherin and the cytoplasmic accumulation of β-catenin.[8] Furthermore, nuclear β-catenin can induce the expression of B-cell lymphoma 9 (BCL9) and B-cell lymphoma 9-like (BCL9L), which inducing tumor proliferation and survival.[9]

BCL9 protein coded by BCL9 gene which located on chromosome 1q21 often involved in secondary chromosomal abnormalities, which connect ygopus and β-catenin[10] is absent expressed normal tissues,[11] and the overexpression of BCL9 contributes to the tumor proliferation, recurrence, progression, and metastasis in colorectal cancer, multiple myeloma, hepatocellular carcinoma and breast cancer, and BCL9 knockdown can effectively increase the survival of xenograft mice.[12–14] This evidence confirms the involvement of BCL9 in tumor progression, underscoring its relevance as a new therapeutic target for cancers associated with Wnt activation. However, the value of BCL9 and the molecular mechanism of action of BCL9 in PTC have not been studied. In this study, we explored the expression, prognostic value, and mechanism of BCL9 in PTC.

Materials and Methods

Dataset

The gene expression data of 512 tumor samples (including 499 PTC samples) and 59 normal samples were downloaded from The Cancer Genome Atlas (TCGA) database. The UCSC Xena project (http://Xena.ucsc.edu/) (download in July 2022). A total of 499 PTC samples and 59 normal samples were enrolled in our study.

HPA

We studied BCL9 protein expression in PTC using The Human Protein Atlas. The Human Protein Atlas (HPA) (https://www.proteinatlas.org/) focusses on a particular aspect of the genome-wide analysis of the human proteins.

PTC Tissues and Adjacent Tissues

The tissues containing 59 PTC tissues and paired normal thyroid tissues were collected. BCL9 mRNA expression of 59 PTC and normal thyroid tissues were tested by qRT-PCR. The protein expression of BCL9 in 12 PTC and normal thyroid tissues were tested by immunohistochemistry. The study was agreed with the ethics committee (No. 2020S181) and all patients agreed to use their tissues, which complied with the Declaration of Helsinki.

qRT-PCR

Total RNA of 59 PTC and normal thyroid tissues was extracted by TRIzol reagent (Invitrogen). A high-capacity cDNA synthesis kit (Takara Bio, Inc, Kusatsu, Shiga, Japan) was used to make cDNA from 2 μg total RNA in 30 μL of reaction buffer, according to the manufacturer's instructions. The thermal cycling conditions were 95°C for 1 min, followed by 40 cycles of 95°C for 10s and 60°C 40s. The mRNA of BCL9 was then tested in triplicate by SYBR Green qPCR Mix (Toyobo, Shanghai, China). Primer sequences of BCL9 were as follow: Forward: 5' - ACACACCACACTCGATGACC - 3', Reverse: 5' - AGCTTCTGCAGCTTTATTGGC - 3'. Primer sequences of internal control-GAPDH were as follow: Forward: 5' - GAG AAGGCTGGGGCTCATTT - 3', Reverse: 5' - TAAGCAGTTGGTGGTGCAGG - 3'. Relative mRNA expression was worked out using the $2^{-\Delta\Delta CT}$ method.

Immunohistochemistry (IHC)

BCL9 protein expression of 12 PTC and normal thyroid tissues were tested by immunohistochemistry. BCL9 protein antibody (anti-BCL9) (Product PA5-93229) was obtained from ThermoFisher Scientific, China. Anti-BCL9 protein antibody diluted 1:100 was used to immunohistochemistry. The IHC image under a pathology imaging system microscope (Akoya Biosciences, California) blinded to clinical information were independently assessed by two pathologists who scored using inForm software (V.2.4.2; Akoya Biosciences). The percent score of positive cells was assessed as follow: 0 (0–5%), 1 (6–25%), 2 (26–50%), 3 (51–75%), 4 (>75%). The staining intensity was assessed as follows: 0 for no color, 1 for yellow, 2 for light brown, and 3 for dark brown. The outcome of final staining score was defined as the multiplication of percentage and intensity scores: 0 (negative), I (1–4), II (5–8), and III (9–12). For a further statistical

analysis, we defined a low protein expression group for score of 0 or I, while scores of II or III were severed as a high protein expression group.

Cell Culture and Treatment

Human papillary thyroid cancer cell lines (PTC-1, K1 and TPC1) and normal thyroid cells (HTori-3 Cell) were bought from Shanghai Institute of Cell Biology (Shanghai, China). All cell lines were grown in a 5% CO_2 ThermoFisher incubator. We use STR to identify and compare all purchased cell lines to reliable databases.

Lipo3000 transfection reagent (Invitrogen, USA) was mixed with siRNA (Small interfering RNA) to transfect PTC cells. Media was removed 48 hours after transfection. The sequences of the siBCL9 were as follows: siBCL9#1 sense: GCCAGGUUGAAACUAUCGU(dT) (dT), siBCL9#2 sense: GGACAUCCCUCUUGGUACA(dT)(dT).

CCK8 Assay

Cells from each experimental group in the logarithmic growth phase and in good growth conditions were digested and resuspended in full culture media. Cells were seeded at 3000 papillary thyroid cancer cells per well in 96-well plates was measured using the Cell Counting Kit-8 (Invitrogen, USA) according to the manufacturer's instructions at 24 h, 48 h, 72 h, and 96 h. The optical density values at 450 nm were measured using an enzyme marker (Molecular Devices, Rockford, IL, USA).

Colony-Formation Assay

Three thousand papillary thyroid cancer cells were seeded into six-well plates and cultured for 14 days. Crystal violet (Beyotime, China) was used to dye the cell colonies after they had been fixed for 10 minutes in 4% polyacetal. The cell colonies were photographed and counted. First, we used Image J software to process cloned images. Then, we converted them into grayscale images and selected lower cutting values to obtain the data. Finally, we counted the relative strength of cell proliferation ability in experimental group and control group by the same cutting values.

Transwell Assay

2×10^4 papillary thyroid cancer cells are seeded in the upper chamber of a transwell chamber in a 24-well plate (Corning, USA). After 24 hours of incubation at 37°C, the cells were wiped from the top surface of the chamber. Cells on the bottom surface of the chambers were fixed with 4% paraformaldehyde for 10 minutes before being stained with crystal violet for 10 minutes (Beyotime, China). The number of migrating cells under the Olympus CellSens Dimension software at 100× magnification was counted and photographed using Image J software.

Scratch Assay

Papillary thyroid cancer cells in the log phase of growth were placed in 24-well plates with IBIDI two-well culture inserts and incubated for 24 hours. Forceps were used to carefully remove the culture implants from the pristine table. Each well received 1 mL of low-serum media, and the rate of cell migration was analyzed according to the healed area of the scratch under the Olympus CellSens Dimension software at 100× magnification.

Co-Expressed Genes Analysis and Functional Enrichment Analyses

The Pearson correlation coefficient (r) was applied to find BCL9 co-expressed genes and the screening threshold was P <0.001 and |r| >0.6 by R software. We also estimated the correlation between BCL9 and the key gene of Wnt/β-catenin and MAPK pathway by using the "correlation module" of The Tumor Immune Estimation Resource (TIMER) database.[15] Differentially expressed genes (DEGs) between low and high BCL9 groups by the median expression were screened by using "limma" and "DESeq2" package in R software on the basis of the thresholds of | log2FoldChange| >1 and adjusted P-value (padj) <0.05. Gene Ontology (GO) and Kyoto Encyclopedia of Genes and Genomes (KEGG) enrichment analyses were performed to analyze the function of BCL9 through "clusterProfiler" package. "clusterProfiler" package (4.4.4) was used for GSEA (Gene Set Enrichment Analysis) to elucidate the potential regulatory mechanisms through the analysis of the functional differences based on the low and high BCL9 groups, which identified by adjusted P value <0.05.

Correlation Between BCL9 and Tumor Immune Microenvironment

The relationship between tumor cells and tumor immune microenvironment (TIME) is well recognized as a key clinical feature in multiple malignant tumors. With the CIBERSORT L22 as the reference, we analyzed the mRNA expression matrix using CIBERSORT R script acquired from the CIBERSORT website (https://cibersortx.standard.edu/). By using Monte Carlo sampling, we calculated an empirical P-value for the deconvolution of each case. To obtain the scores of multiple immunocytes, the gene expression matrix was analyzed via "estimate" package and the correlation heatmaps between immune checkpoint genes and BCL9 were visualized via "corrplot" package.

Protein–Protein Interaction Analysis

String (https://string-db.org/) database was used to construct the protein–protein interaction network (PPI) of BCL9.

Statistical Analysis

The difference of BCL9 in PTC tissues and normal thyroid tissues from TCGA databases were calculated by the Wilcoxon rank-sum test. Survival analysis was performed by the Log rank test. The difference of PTC tissues between the low and high BCL9 expression groups was calculated by the Spearman's analysis. The risk factors of neck lymph node metastasis were calculated by logistic regression analysis. Data were processed through R (V.4.1.3), SPSS version 25.0, and GraphPad Prism (V.9.0) software. P value <0.05 was considered statistically significant, $*P < 0.05$, $**P < 0.01$, $***P < 0.001$.

Results

The Expression and Clinical Significance of BCL9 in PTC

To investigate the clinical significance of BCL9 in PTC, we analyzed the relationship between its expression levels and clinical value. First, we investigated the expression of BCL9 in PTC, the mRNA expression level of BCL9 was significantly higher significantly in PTC than in normal tissues (Figure 1A and B). To investigate the prognostic value of BCL9 in PTC, the PTC samples from the TCGA database were divided into low BCL9 (n = 250) and high BCL9 (n = 249), on the base of the median of BCL9 expression level. KM survival analysis showed that the PFS of PTC group with high BCL9 was shorter ($P = 0.049$) compared with PTC group with low BCL9 (Figure 1C). To determine the clinical significance of BCL9 in PTC, the differences in clinical data between the low and high BCL9 groups were investigated by Spearman's analysis and the high BCL9 group correlated to lymph node metastasis ($P < 0.001$) (Figure 1D).

Validation of BCL9 Expression in the HPA Database and in PTC Tissues by qRT-PCR and IHC

To go deeply into BCL9 expression in PTC, we investigate the BCL9 expression based on the results from the HPA database, BCL9 exhibited a higher expression in PTC tissues than in normal tissues (Figure 2A). For investigating into the tissue level, we tested BCL9 mRNA expression of 59 paired PTC and adjacent tissues by qRT-PCR and BCL9 protein expression of 12 paired PTC and adjacent tissues by IHC, we found that the mRNA ($P = 0.001$) and protein expression of BCL9 ($P = 0.039$) was significantly overexpressed in PTC than in paired normal thyroid tissues (Figure 2B and C).

BCL9 Correlated with Neck Lymph Nodes Metastasis in PTC

To investigate the relationship between BCL9 expression and PTC clinicopathological characteristics, we divided 59 PTC patients into low and high BCL9 mRNA expression groups based on the median expression. High BCL9 level was associated with a more advanced N stage ($P = 0.024$) (Table 1). Neck lymph node metastasis might be associated with high BCL9 expression.

BCL9 Was a Risk Factor of Neck Lymph Nodes Metastasis in PTC

In order to investigate the risk factors of neck lymph nodes metastasis, we performed a logistic regression analysis. According to the status of neck lymph nodes metastasis, the group with lymph nodes metastasis had larger tumor size

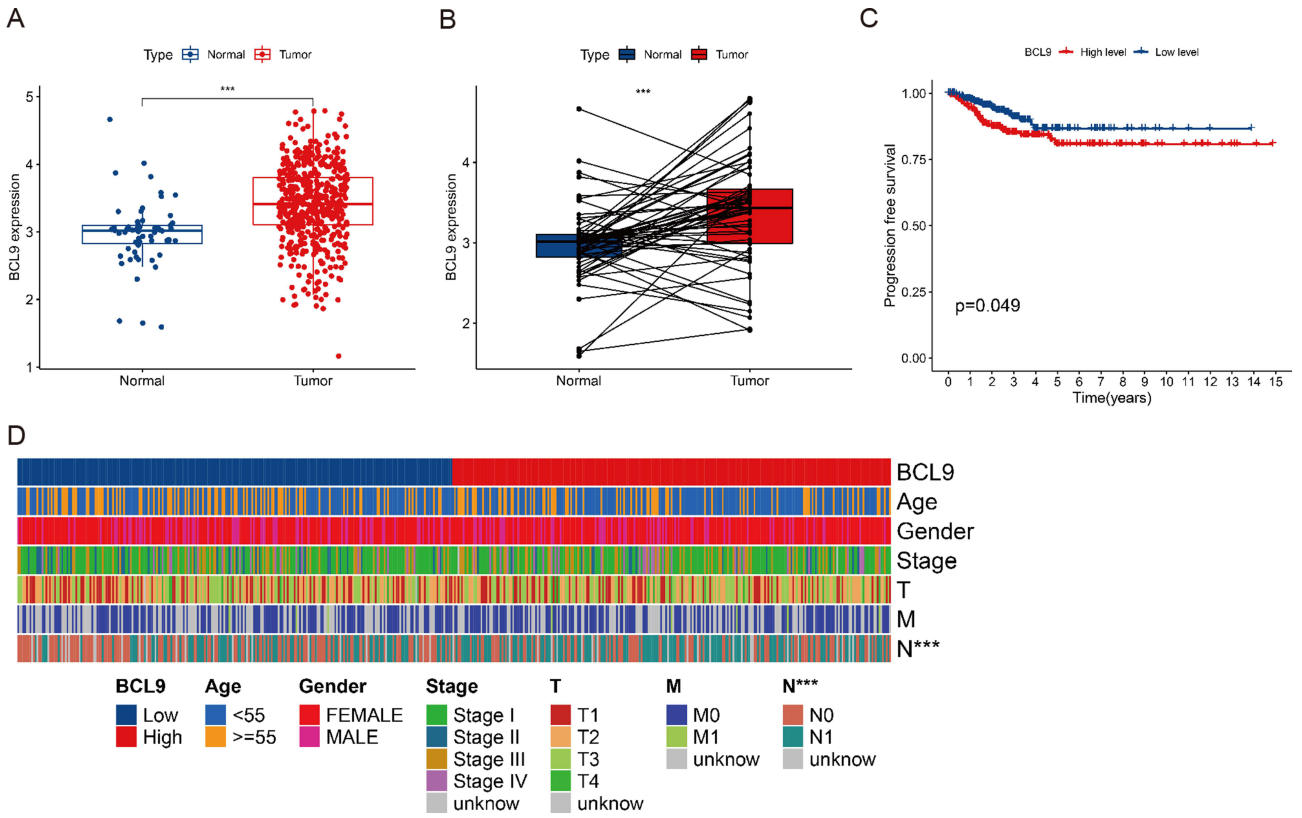

Figure 1 Analysis of the BCL9 expression based on the TCGA database. (**A**) BCL9 was significantly higher expressed in PTC. (**B**) BCL9 was significantly higher expressed in paired PTC. (**C**) BCL9 was associated with poorer PFS of PTC patients. (**D**) BCL9 was associated with clinical characteristics of PTC patients and high BCL9 group significantly correlated to lymph node metastasis. ***P <0.001.
Abbreviations: Normal, normal thyroid tissues; Tumor, papillary thyroid tumor tissues.

(P = 0.026) and higher BCL9 expression (P = 0.024) (Table 2). What's more, tumor size (OR = 3.940, P = 0.027) and BCL9 (OR = 3.770, P = 0.025) were positively correlated with neck lymph nodes metastasis in PTC patients (Table 3).

BCL9 Was Overexpressed in Various PTC Cell Lines and Promotes PTC Cell Proliferation and Invasion

BCL9 expression was significantly higher in TPC-1, K1, and KTC1 cells than in thyroid cells (HTori-3 Cell) by qRT-PCR (Figure 3A). In order to confirm the role of BCL9 in PTC cell lines through cell experiments, we chose TPC-1 and K1 cell lines with the most obvious BCL9 overexpression and knocked it out, then verified the knockdown efficiency (Figure 3B and C). CCK8 (Figure 3D and E) and colony assay (Figure 4A and B) results showed that BCL9 knockdown significantly inhibited TPC-1 and K1 cell proliferation. Furthermore, the transwell assay (Figure 4C and D) and scratch assay (Figure 4E–G) demonstrated that BCL9 knockdown significantly inhibited the invasive ability of PTC cells.

The Biological Functions of BCL9 in PTC

In order to further investigate the underlying molecular mechanisms, we conducted bioinformatics analysis to explore the potential pathways and the relationship with immune infiltration involved in BCL9. We performed the co-expression analysis based on the data of the TCGA cohort to elucidate genes that interact closely with BCL9. It has been shown that the top 5 genes negatively correlated with BCL9 were SNTA1, CHCHD10, PRADC1, VEGFB, and GCAT, and the top 5 genes positively correlated with BCL9 were KDM5B, NRIP1, MAP3K1, NAV2, and PIAS3 (Figure 5A). GO functional enrichment analysis was performed for top 5 negative and positive co-expressed genes. The top 6 association with biological process (BP) included GO:0060048: cardiac muscle contraction, GO:0006941: striated muscle contraction, GO:0050679: positive regulation of epithelial cell proliferation, GO:0002551: mast cell chemotaxis, GO: 0033234: negative regulation of protein sumoylation,

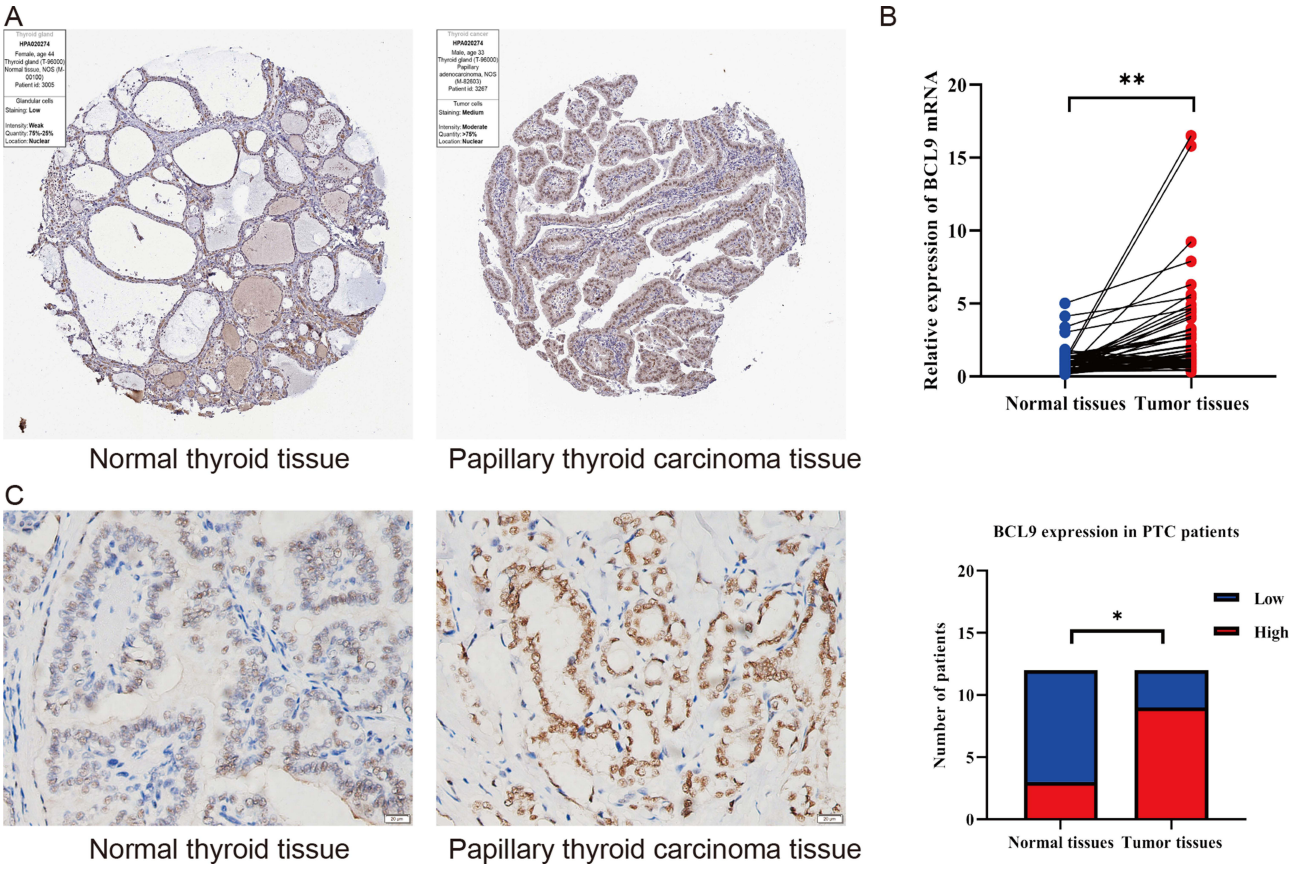

Figure 2 The BCL9 expressed highly in PTC. (**A**) The protein of BCL9 was higher expressed in PTC by the HPA database. (**B**) The mRNA of BCL9 was higher expressed in PTC by qRT-PCR. (**C**) The protein of BCL9 was higher expressed in PTC by IHC. *P <0.05, **P <0.01.

GO:2000169: regulation of peptidyl-cysteine S-nitrosylation. Cellular components (CC) included GO:0016607: nuclear speck, GO:0005614: interstitial matrix, GO:0016010: dystrophin-associated glycoprotein complex, GO:0090665: glycoprotein complex, GO:0005743: mitochondrial inner membrane, GO:0016328: lateral plasma membrane. Molecular function

Table 1 The Patients' Clinicopathological Characteristics Analyzed Based on Median of BCL9 mRNA

Characteristics	Low (n=30)	High (n=29)	Chi-square	*P* value
Age (years)			0.004	0.948
< 55	24	23		
≥ 55	6	6		
Sex			0.203	0.706
Female	27	25		
Male	3	4		
T stage			0.036	0.850
≤ 1cm	10	9		
> 1cm	20	20		
N stage			5.107	0.024*
N0	17	8		
N1	13	21		
$BRAF^{V600E}$			0.894	0.344
Negative	7	10		
Positive	23	19		

Note: *P < 0.05.

Table 2 Risk Factors of Lymph Nodes Metastasis in Papillary Thyroid Carcinoma

Characteristics	Lymph Node Metastasis (n=34)	Non-Metastasis (n=25)	Chi-square	*P* value
Age (years)			3.641	0.1
< 55	30	17		
≥ 55	4	8		
Sex			0.710	0.443
Female	31	21		
Male	3	4		
T stage			4.958	0.026*
≤ 1cm	7	12		
> 1cm	27	13		
$BRAF^{V600E}$			1.092	0.386
Negative	8	9		
Positive	26	16		
BCL9			5.107	0.024*
Low	13	17		
High	21	8		

Note: *$P < 0.05$.

Table 3 Logistic Regression Analysis for the Risk Factor of Neck Lymph Node Metastasis

Variables	B	SE	Walds	P	OR	95% CI
T (>1cm vs ≤1cm)	1.371	0.622	4.864	0.027*	3.940	1.165–13.325
BCL9 (High vs Low)	1.327	0.590	5.052	0.025*	3.770	1.185–11.990

Note: *$P < 0.05$.
Abbreviations: OR, Odd ratio, CI, Confidence interval.

(MF) included GO:0008201: heparin binding, GO:0003714: transcription corepressor activity, GO:0050998: nitric-oxide synthase binding, GO:0035259: nuclear glucocorticoid receptor binding, GO:0005172: vascular endothelial growth factor receptor binding, GO:0005539: glycosaminoglycan binding (Figure 5B).

Subsequently, 1066 DEGs including 471 up-regulated and 595 down-regulated were identified statistically significantly (|log fold change (logFC)| > 1, $P < 0.05$). The top 50 up-regulated DEGs and top 50 down-regulated DEGs were illustrated by the heatmap (Figure 5C).

To go deeply into the function of 1066 DEGs between high and low expression of BCL9 in PTC, GO and KEGG functional enrichment analysis were performed. The top 10 association with BP included detoxification of copper ion, stress response to copper ion, cellular response to zinc ion, stress response to metal ion, detoxification of inorganic compound, cellular zinc ion homeostasis, zinc ion homeostasis, cellular response to copper ion, response to copper ion, and response to zinc ion. CC included ion channel complex, transmembrane transporter complex, transporter complex, postsynaptic membrane, synaptic membrane, cation channel complex, juxtaparanode region of axon, potassium channel complex, voltage-gated potassium channel complex, and chloride channel complex. MF included sulfur compound binding, glycosaminoglycan binding, heparin binding, passive transmembrane transporter activity, channel activity, receptor ligand activity, signaling receptor activator activity, chloride transmembrane transporter activity, growth factor activity, and ion channel activity (Figure 5D). The top 10 KEGG pathways included neuroactive ligand–receptor interaction, mineral absorption, nicotine addiction, PPAR signaling pathway, thyroid hormone synthesis, gastric acid secretion, cAMP signaling pathway, pancreatic secretion, cocaine addiction, and proximal tubule bicarbonate reclamation (Figure 5E).

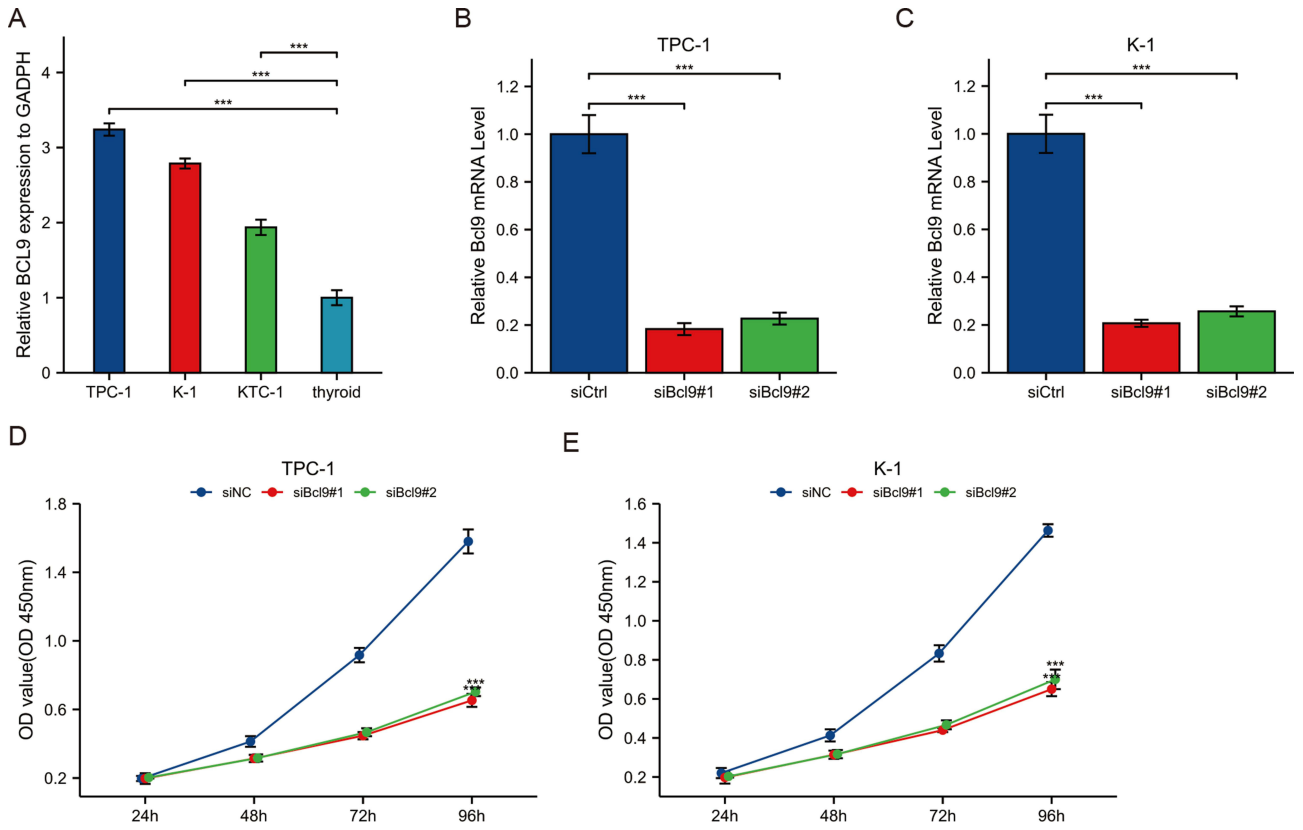

Figure 3 BCL9 was overexpressed in PTC cell lines. (**A**) BCL9 expression was significantly higher in TPC-1, K1, and KTC1 cells than in normal thyroid cells by qRT-PCR. (**B** and **C**) The expression of BCL9was downregulated in TPC-1 (**B**) and K1 (**C**). (**D** and **E**) Knockdown of BCL9 significantly inhibited TPC-1 (**D**) and K1 (**E**) cell proliferation by CCK8 assay. ***P <0.001.

Abbreviations: siCtrl, small interfering Control; siNC, small interfering Negative Control.

GSEA analysis was performed to acquire a greater depth of understanding of the involved pathways. Significant differences (FDR < 0.05, adjusted $P < 0.05$) were observed in the enrichment of MSigDB Collection (c2.cp.kegg.v7.4.symbols.gmt and c5.go.v7.4.symbols.gmt) of these pathways – focal adhesion, tight junction, olfactory transduction, oxidative phosphorylation, and Parkinson's disease (Figure 5F). These results suggested that BCL9 participated in focal adhesion and tight junction of PTC.

BCL9 Was Related with Wnt/β-Catenin and MAPK Pathway

Some researcher supported activation of the mitogen-activated protein kinase (MAPK) pathway and Wnt/β-catenin signaling pathway[8,9] were widely accepted in mediating PTC cell proliferation and migration. We investigated the relationship between BCL9 and Wnt/β-catenin, as well as MAPK pathway in PTC based on the "correlation module" of the TIMER database. As shown in Figure 6, BCL9 was significant positively associated with the key genes of Wnt/β-catenin pathway-Wnt2 ($r = 0.208$, $P = 2.32E-06$), 2B ($r = 0.392$, $P = 4.25E-20$), 3 ($r = 0.532$, $P = 1.82E-38$), 5A ($r = 0.538$, $P = 1.3E-39$), 7A ($r = 0.158$, $P = 3.52E-04$), 7B ($r = 0.2$, $P = 5.34E-06$), 8A ($r = 0.195$, $P = 8.91E-06$), 8B ($r = 0.226$, $P = 2.71E-07$), 9A ($r = 0.273$, $P = 3.56E-10$), 9B ($r = 0.316$, $P = 2.73E-13$), 10A ($r = 0.474$, $P = 1.7E-30$), 16 ($r = 0.169$, $P = 1.28E-04$) and CTNNB1 ($r = 0.681$, $P = 1.34E-70$), and positively correlated with the key molecule of MAPK pathway ($r = 0.547$, $P = 4.28E-41$).

The Correlation Between BCL9 and Tumor Immune Microenvironment

Tumor-infiltrating immune cells (TICs) were widely existed in the TIME (tumor immune microenvironment) of PTC and affected pathological processes, and PTC samples in the TCGA database were subdivided into high and low BCL9 sets on the base of BCL9 median expression level. StromalScore and ESTIMATEScore of high-BCL9 group were generally higher when compared with those of low BCL9 group by the ESTIMATE algorithm evaluation (Figure 7A). Next, we investigated the

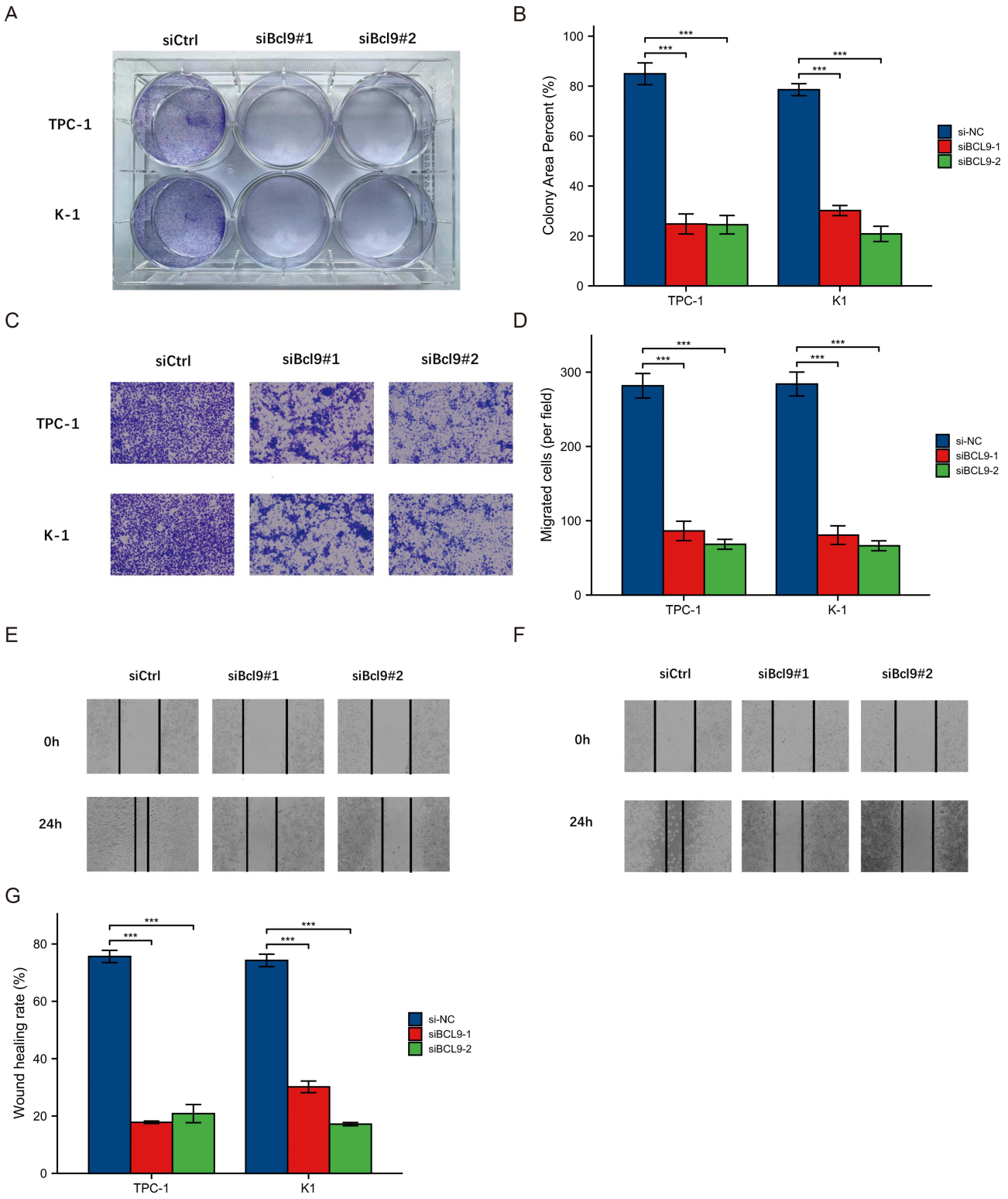

Figure 4 Knockdown of BCL9 significantly inhibited proliferation and invasion of PTC cells. (**A** and **B**) Colony assay showed that BCL9 knockdown significantly inhibited TPC-1 and K1 cell proliferation. (**C** and **D**) Transwell assay showed that BCL9 knockdown significantly inhibited the invasion of TPC-1 (**C**) and K1 (**D**) cells. (**E**–**G**) Scratch assay showed that BCL9 knockdown significantly inhibited the invasion of TPC-1 (**E**) and K1 (**F**) cells. ***P <0.001.

Abbreviations: siCtrl, small interfering Control; siNC, small interfering Negative Control.

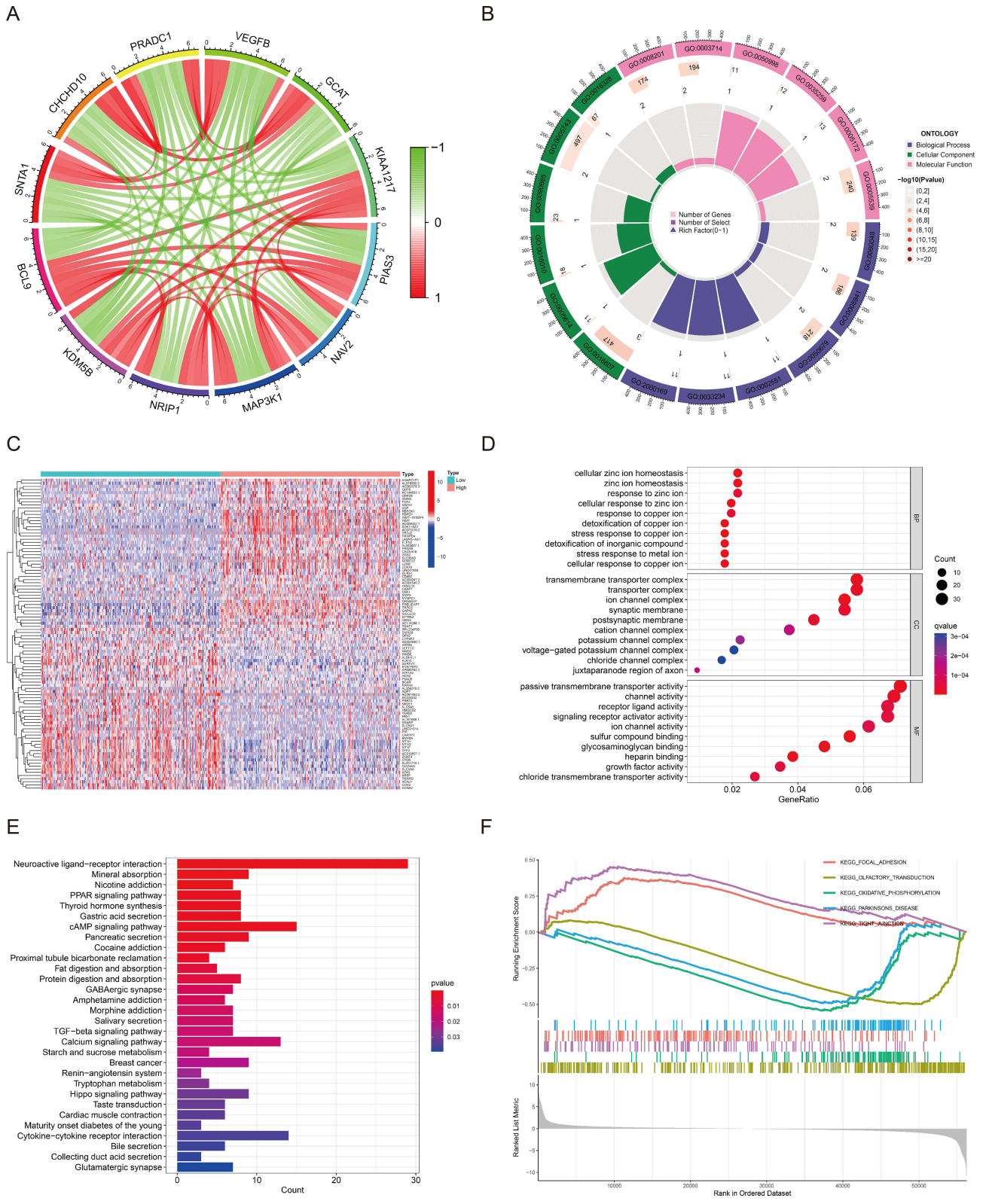

Figure 5 Functional annotation of BCL9. (**A**) Co-expression genes based on BCL9 expression. (**B**) GO enrichment analyses of Co-expression genes. (**C**) Differentially expressed genes (DEGs) between high and low BCL9 expression groups. (**D**) GO enrichment analyses of DEGs. (**E**) KEGG enrichment analysis of DEGs. (**F**) GSEA analysis to investigate the potential regulatory mechanisms.

Abbreviations: GO, gene ontology; KEGG, kyoto encyclopedia of genes and genomes; GSEA, gene set enrichment analysis.

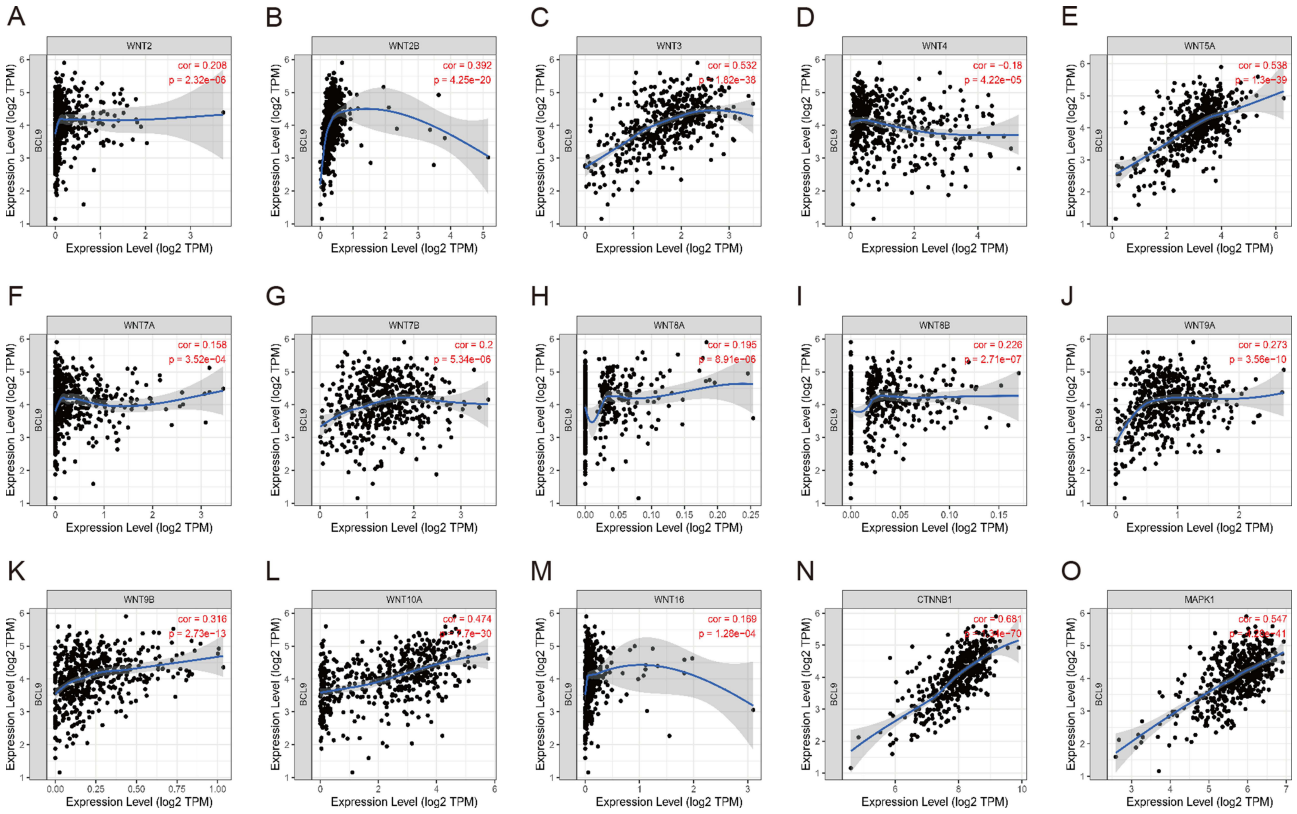

Figure 6 BCL9 was positively correlated with the activation states of Wnt/β-catenin and MAPK pathway. (**A**–**M**) Wnt ligands - Wnt2, 2B, 3, 4, 5A, 7B, 8A, 8B, 9A, 9B, 10A, 16. (**N**) CTNNB1, β-catenin gene. (**O**) MAPK1.
Abbreviations: cor, correlation; TPM, transcripts per million; CTNNB1, catenin beta 1; MAPK1, mitogen-activated protein kinase 1.

relationship between BCL9 expression and various TIC subtypes, and the differences in the proportion of 22 types of TICs in tumor tissues for the high- and low-BCL9 expression groups were shown in lollipop plots. We discovered that CD4 memory resting T cells, M0 macrophages, and mast cells resting were positively associated with BCL9 expression, and CD8 T cells, activated dendritic cells, neutrophils, and activated NK cells were negatively associated with BCL9 expression, suggesting that BCL9 affected PTC prognosis by influencing the immune status of the TIME (Figure 7B). In addition, BCL9 was positively associated with mRNA of immune checkpoint genes, such as CD274 (PD-L1 code gene) (r = 0.118, P = 0.008), CD276 (r = 0.504, P = 8.20E-34), CD44 (r = 0.486, P = 3.57E-31), TNFRSF8 (r = 0.410, P = 8.23E-22), TNFSF15 (r = 0.333, P = 1.68E-14), CD40 (r = 0.311, P = 9.10E-13) and negatively associated with the transcription levels of immune checkpoint genes, such as IDO2 (r = −0.219, P = 7.21E-07), TNFRSF4 (r = −0.133, P = 0.003), IDO1 (r = −0.130, P = 0.003), CD27 (r = −0.100, P = 0.025), TNFRSF14 (r = −0.99, P = 0.027) (Figure 7C). But BCL9 expression was not correlated with tumor mutation burden (TMB) in PTC (Figure 7D). In conclusion, BCL9 was associated with inhibition of cytotoxic immune cells (CD8+ T and NK cells) infiltration and promotion of anti-cancer immune PD-L1 expression.

Protein–Protein Interaction of BCL9

We guessed BCL9 promoted the expression of anti-tumor immune PD-L1 through Wnt/β-catenin or MAPK pathway. To further investigate the relationship among BCL9, β-catenin, MAPK1, and PD-L1, we constructed the PPI network and found that BCL9 was closely associated with β-catenin proteins (coded by CTNNB1 (Catenin Beta 1)) and β-catenin proteins (coded by CTNNB1) were closely associated with PD-L1 (coded by CD274) and MAPK1 (Mitogen-activated protein kinase 1) in Figure 8.

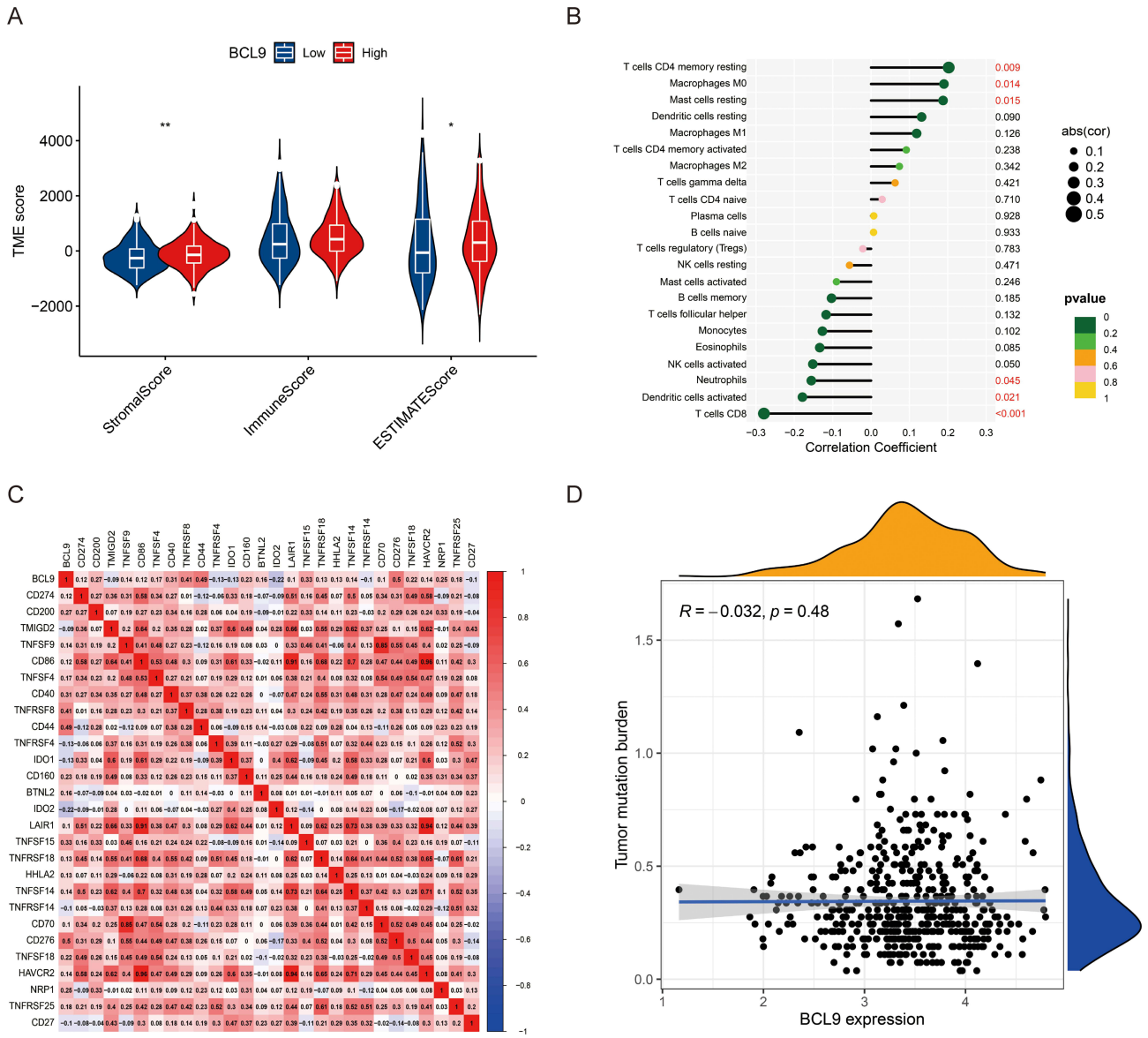

Figure 7 The relationship among tumor immune microenvironment, tumor-infiltrating immune cells, immune checkpoint genes, and BCL9 expression. (**A**) The correlation between BCL9 expression and TIME in PTC. (**B**) The correlation between BCL9 expression and various types of tumor-infiltrating immune cells in PTC. (**C**) The heatmaps of correlation between BCL9 expression and immune checkpoint genes. (**D**) The relationship between BCL9 expression and tumor mutation burden (TMB) in PTC. **P* <0.05, ***P* <0.01.

Abbreviations: TME score, tumor microenvironment score; R, relationship.

Discussion

The preoperative diagnosis of PTC patients mainly relies on Fine-needle aspiration cytology (FNAC) of thyroid nodules. The Bethesda classification system for reporting thyroid cytopathology is the criterion for interpreting fine needle aspirate (FNA). Incidental thyroid malignancy which almost PTC was found in 1.53% cases of Bethesda II and 18–20% cases of Bethesda III. More than 80% of Bethesda types II and III may not require surgery, and to avoid unnecessary surgery for patients with thyroid nodules, more molecular markers for PTC are needed to improve the diagnosis rate of malignancy for Bethesda II and III.[16,17] PTC is a low-grade malignant tumor with relatively satisfactory prognosis, while accounts for the vast majority of thyroid malignancies, but the neck lymph node metastasis and recurrence are still unavoidable. The frequency of neck lymph node metastasis (LNM) is 30–90% in PTC.[18] In addition, LNM acts as an important factor for recurrence.[19] The revised American Thyroid Association management guidelines suggest that neck LNM is considered a risk factor for prognosis in PTC patients.[20] The criterion for high risk in post-operative risk assessment is ≥5 lymph

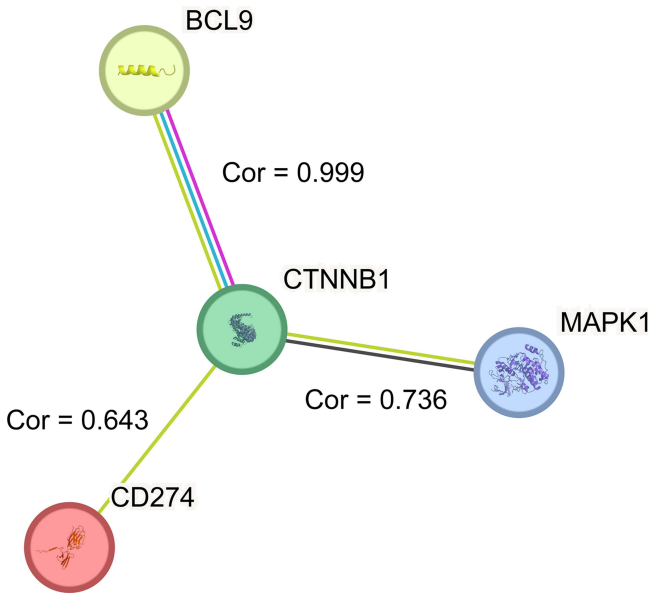

Figure 8 The correlation among BCL9, β-catenin proteins (coded by CTNNB1), PD-L1 (coded by CD274), and MAPK1. The correlation (cor) between BCL9 and β-catenin (coded by CTNNB1) was 0.999, and β-catenin was closely associated with PD-L1 (coded by CD274) (cor = 0.643) and MAPK1 (cor = 0.736).
Abbreviations: Cor, correlation; CTNNB1, catenin beta 1; MAPK1, mitogen-activated protein kinase 1.

node metastases,[21] and the ratio of the metastatic lymph node count to the total lymph node yield (MLNR) has also been reported as a valuable prognostic indicator in PTC.[22,23] It remains a challenge to accurately identify PTC patients diagnosed in Bethesda II and III after FNAC and PTC patients with higher risk of recurrence and metastasis. In this study, we found that BCL9 was overexpressed (Figures 1–3A) and positively correlated with neck lymph nodes metastasis (*OR* = 3.770, *P* = 0.025) in PTC patients (Table 3).

Some researcher supported PTC has constitutive activation of the MAPK pathway,[24] in our study, we verified BCL9 was related to MAPK1 ($r = 0.547$, $P < 0.001$) (Figure 6) and MAP3K1 (Figure 5A). While the activation of the MAPK and PI3K/Akt pathways caused by BRAFV600E mutation, RAS mutation or RET mutation is the major pathogenic mechanism in thyroid cancer,[25] however, the canonical Wnt signaling pathway plays an irreplaceable role as well.[26] Recent researchers found that BRAFV600E, RAS and RET mutation can stimulate the Wnt pathway to promote tumorigenesis.[27] Signaling by Wnt proteins activates β-catenin-independent or β-catenin-dependent pathway. When proteins of the family-Wnt1/3/3a/7A/10B bound to a frizzled receptor and the LDL-Receptor-related protein coreceptor, Wnt/β-catenin pathway could be activated. The study has found that BCL9/9L promoted cell proliferation and metastasis through the activating β-catenin.[28] In order to investigate whether the mechanism existed in PTC, we analyzed the correlations between BCL9 and Wnt/β-catenin by using the "correlation" module of the TIMER database and verified BCL9 was positively related with Wnt2, 2B, 3, 5A, 7A, 7B, 8A, 8B, 9A, 9B, 10A, 16 and CTNNB1 (Figure 6).

Immune cell infiltration has been reported to be related to prognosis in patients with PTC,[29] and the antitumor effect of autoimmunity may be another important mechanism.[30] The Wnt/β-catenin pathway has also been identified as an important oncogenic regulator of immune evasion.[31,32] Up-expressed immune checkpoint molecules in the tumor immune microenvironment play a critical role in antitumor immunity evasion and cancer progression.[33] In our study, we found that the overexpression of BCL9 was related to the proportion of StromalScore in the TIME in PTC (Figure 7A) and T cells CD8 and NK cells activated which acted as anti-tumor immune cells were negatively correlated with BCL9 expression (Figure 7B). CD8+ T cell abundance was negatively correlated with BCL9 expression in triple-negative breast cancers.[34] Currently, immune checkpoint inhibitors, including anti-cytotoxic T-lymphocyte-associated protein 4 (anti-CTLA4),[35] anti-PD-1,[36] and anti-programmed death-ligand 1 (PD-L1)[37] were permitted for the cancer treatment. BCL9 was identified to be positively related with PD-L1 gene (CD724) expression (Figure 7C). Because BCL9 activated Wnt/β-catenin and MAPK pathway inhibited tumor killing immune cell (CD8 T and NK cells)

infiltration and promoted the expression of anti-tumor immune PD-L1, BCL9 further promoted lymph node metastasis and the poor PFS of PTC (Figure 1C).

Conclusions

By investigating the relationship between BCL9 and PTC, our study found that BCL9 expression was correlated with the poor PFS and several anti-tumor infiltrating immune cells in PTC, which highlighted the prognostic and predictive value of BCL9 in PTC.

However, there were several limitations to this study. We have only verified the expression of BCL9 in PTC, not in other types of thyroid carcinoma such as follicular thyroid carcinoma, medullary thyroid carcinoma (MTC), and anaplastic thyroid carcinoma (ATC). We should go deeper into the impact of BCL9 on Wnt/β-catenin pathway and conduct remedial experiments with Wnt/β-catenin pathway inhibitors. Furthermore, we should confirm that BCL9 could promote PTC progression in vivo and the impact of BCL9 on the tumor immune microenvironment.

Data Sharing Statement

The datasets can be obtained via the two databases (TCGA and HPA) or the first authors on reasonable request.

Ethics Approval and Consent to Participate

The study was approved by the ethics committee of Tongji Hospital affiliated with Tongji Medical College of Huazhong University of Science and Technology (approval No. 2020S181). Informed consent was provided by all patients. All experiments were performed in accordance with the Declaration of Helsinki.

Acknowledgments

This paper has been uploaded to ResearchGate as a preprint: https://www.researchgate.net/publication/372453277_BCL9_is_a_risk_factor_of_neck_lymph_nodes_metastasis_and_correlated_with_immune_cell_infiltration_in_papillary_thyroid_carcinoma. The results of the present study were in part based on data from TCGA. We are grateful to Dr. Zhengwei Gui (Tongji Hospital affiliated with Tongji Medical College of Huazhong University of Science and Technology) for his help with the experiments in this study. Rui Zhang and Zhengwei Gui are co-first authors.

Author Contributions

All authors made a significant contribution to the work reported, whether that is in the conception, study design, execution, acquisition of data, analysis and interpretation, or in all these areas; took part in drafting, revising or critically reviewing the article; gave final approval of the version to be published; have agreed on the journal to which the article has been submitted; and agree to be accountable for all aspects of the work.

Funding

This work was supported by Special funds for scientific and technological development of Hubei Province (2022BGE233).

Disclosure

The authors declare that the research was conducted in the absence of any commercial or financial relationships that could be construed as a potential conflict of interest.

References

1. Siegel RL, Miller KD, Jemal A. Cancer statistics, 2020. *CA Cancer J Clin*. 2020;70:7–30. doi:10.3322/caac.21590
2. Ghossein R, Livolsi VA. Papillary thyroid carcinoma tall cell variant. *Thyroid*. 2008;18:1179–1181. doi:10.1089/thy.2008.0164
3. Dong W, Horiuchi K, Tokumitsu H, et al. Time-varying pattern of mortality and recurrence from papillary thyroid cancer: lessons from a long-term follow-up. *Thyroid*. 2019;29:802–808. doi:10.1089/thy.2018.0128
4. Cibas ES, Ali SZ. The 2017 Bethesda system for reporting thyroid cytopathology. *Thyroid*. 2017;27:1341–1346. doi:10.1089/thy.2017.0500
5. Nusse R, Clevers H. Wnt/beta-catenin signaling, disease, and emerging therapeutic modalities. *Cell*. 2017;169:985–999. doi:10.1016/j.cell.2017.05.016

6. Wang X, Lu X, Geng Z, Yang G, Shi Y. LncRNA PTCSC3/miR-574-5p governs cell proliferation and migration of papillary thyroid carcinoma via Wnt/beta-catenin signaling. *J Cell Biochem*. 2017;118:4745–4752. doi:10.1002/jcb.26142
7. Yu S, Cao S, Hong S, et al. miR-3619-3p promotes papillary thyroid carcinoma progression via Wnt/beta-catenin pathway. *Ann Transl Med*. 2019;7:643. doi:10.21037/atm.2019.10.71
8. Dong W, Zhang H, Li J, et al. Estrogen induces metastatic potential of papillary thyroid cancer cells through estrogen receptor alpha and beta. *Int J Endocrinol*. 2013;2013:941568. doi:10.1155/2013/941568
9. Liu J, Pan S, Hsieh MH, et al. Targeting Wnt-driven cancer through the inhibition of Porcupine by LGK974. *Proc Natl Acad Sci U S A*. 2013;110:20224–20229. doi:10.1073/pnas.1314239110
10. Kramps T, Peter O, Brunner E, et al. Wnt/wingless signaling requires BCL9/legless-mediated recruitment of pygopus to the nuclear beta-catenin-TCF complex. *Cell*. 2002;109:47–60. doi:10.1016/s0092-8674(02)00679-7
11. Gay DM, Ridgway RA, Muller M, et al. Loss of BCL9/9l suppresses Wnt driven tumourigenesis in models that recapitulate human cancer. *Nat Commun*. 2019;10:723. doi:10.1038/s41467-019-08586-3
12. Mani M, Carrasco DE, Zhang Y, et al. BCL9 promotes tumor progression by conferring enhanced proliferative, metastatic, and angiogenic properties to cancer cells. *Cancer Res*. 2009;69:7577–7586. doi:10.1158/0008-5472.CAN-09-0773
13. de la Roche M, Worm J, Bienz M. The function of BCL9 in Wnt/beta-catenin signaling and colorectal cancer cells. *BMC Cancer*. 2008;8:199. doi:10.1186/1471-2407-8-199
14. Elsarraj HS, Hong Y, Valdez KE, et al. Expression profiling of in vivo ductal carcinoma in situ progression models identified B cell lymphoma-9 as a molecular driver of breast cancer invasion. *Breast Cancer Res*. 2015;17:128. doi:10.1186/s13058-015-0630-z
15. Li T, Fan J, Wang B, et al. TIMER: a web server for comprehensive analysis of tumor-infiltrating immune cells. *Cancer Res*. 2017;77:e108–e110. doi:10.1158/0008-5472.CAN-17-0307
16. Mulita F, Iliopoulos F, Tsilivigkos C, et al. Cancer rate of Bethesda category II thyroid nodules. *Med Glas*. 2022;19(1). doi:10.17392/1413-21
17. Mulita F, Plachouri MK, Liolis E, Vailas M, Panagopoulos K, Maroulis I. Patient outcomes following surgical management of thyroid nodules classified as Bethesda category III (AUS/FLUS). *Endokrynol Pol*. 2021;72(2):143–144. doi:10.5603/EP.a2021.0018
18. Choi YJ, Yun JS, Kook SH, Jung EC, Park YL. Clinical and imaging assessment of cervical lymph node metastasis in papillary thyroid carcinomas. *World J Surg*. 2010;34:1494–1499. doi:10.1007/s00268-010-0541-1
19. Wu X, Gu H, Gao Y, Li B, Fan R. Clinical outcomes and prognostic factors of radioiodine ablation therapy for lymph node metastases from papillary thyroid carcinoma. *Nucl Med Commun*. 2018;39:22–27. doi:10.1097/MNM.0000000000000777
20. Cooper DS, Doherty GM, Haugen BR, et al; American Thyroid Association Guidelines Taskforce on Thyroid N, Differentiated Thyroid C. Revised American Thyroid Association management guidelines for patients with thyroid nodules and differentiated thyroid cancer. *Thyroid*. 2009;19:1167–1214. doi:10.1089/thy.2009.0110
21. Haugen BR. 2015 American Thyroid Association Management Guidelines for adult patients with thyroid nodules and differentiated thyroid cancer: what is new and what has changed? *Cancer*. 2017;123:372–381. doi:10.1002/cncr.30360
22. Kim Y, Roh JL, Gong G, et al. Risk factors for lateral neck recurrence of N0/N1a papillary thyroid cancer. *Ann Surg Oncol*. 2017;24:3609–3616. doi:10.1245/s10434-017-6057-2
23. Nam SH, Roh JL, Gong G, et al. Nodal factors predictive of recurrence after thyroidectomy and neck dissection for papillary thyroid carcinoma. *Thyroid*. 2018;28:88–95. doi:10.1089/thy.2017.0334
24. Sastre-Perona A, Santisteban P. Role of the wnt pathway in thyroid cancer. *Front Endocrinol*. 2012;3:31. doi:10.3389/fendo.2012.00031
25. Xing M. Molecular pathogenesis and mechanisms of thyroid cancer. *Nat Rev Cancer*. 2013;13:184–199. doi:10.1038/nrc3431
26. Saini S, Sripada L, Tulla K, et al. Loss of MADD expression inhibits cellular growth and metastasis in anaplastic thyroid cancer. *Cell Death Dis*. 2019;10:145. doi:10.1038/s41419-019-1351-5
27. Ely KA, Bischoff LA, Weiss VL. Wnt signaling in thyroid homeostasis and carcinogenesis. *Genes*. 2018;9. doi:10.3390/genes9040204
28. Zhao JJ, Carrasco RD. Crosstalk between microRNA30a/b/c/d/e-5p and the canonical Wnt pathway: implications for multiple myeloma therapy. *Cancer Res*. 2014;74:5351–5358. doi:10.1158/0008-5472.CAN-14-0994
29. Cunha LL, Morari EC, Guihen AC, et al. Infiltration of a mixture of immune cells may be related to good prognosis in patients with differentiated thyroid carcinoma. *Clin Endocrinol*. 2012;77:918–925. doi:10.1111/j.1365-2265.2012.04482.x
30. Ehlers M, Schott M. Hashimoto's thyroiditis and papillary thyroid cancer: are they immunologically linked? *Trends Endocrinol Metab*. 2014;25:656–664. doi:10.1016/j.tem.2014.09.001
31. Fu C, Liang X, Cui W, et al. beta-Catenin in dendritic cells exerts opposite functions in cross-priming and maintenance of CD8+ T cells through regulation of IL-10. *Proc Natl Acad Sci U S A*. 2015;112:2823–2828. doi:10.1073/pnas.1414167112
32. Spranger S, Gajewski TF. A new paradigm for tumor immune escape: beta-catenin-driven immune exclusion. *J Immunother Cancer*. 2015;3:43. doi:10.1186/s40425-015-0089-6
33. Francis DM, Manspeaker MP, Schudel A, et al. Blockade of immune checkpoints in lymph nodes through locoregional delivery augments cancer immunotherapy. *Sci Transl Med*. 2020;12. doi:10.1126/scitranslmed.aay3575
34. Jiang YZ, Ma D, Suo C, et al. Genomic and transcriptomic landscape of triple-negative breast cancers: subtypes and treatment strategies. *Cancer Cell*. 2019;35:428–40 e5. doi:10.1016/j.ccell.2019.02.001
35. Michot JM, Bigenwald C, Champiat S, et al. Immune-related adverse events with immune checkpoint blockade: a comprehensive review. *Eur J Cancer*. 2016;54:139–148. doi:10.1016/j.ejca.2015.11.016
36. Rizvi NA, Mazieres J, Planchard D, et al. Activity and safety of nivolumab, an anti-PD-1 immune checkpoint inhibitor, for patients with advanced, refractory squamous non-small-cell lung cancer (CheckMate 063): a Phase 2, single-arm trial. *Lancet Oncol*. 2015;16:257–265. doi:10.1016/S1470-2045(15)70054-9
37. Daver N, Jonas BA, Medeiros BC, Patil U, Yan M. Phase 1b, open-label study evaluating the safety and pharmacokinetics of atezolizumab (anti-PD-L1 antibody) administered in combination with Hu5F9-G4 to patients with relapsed and/or refractory acute myeloid leukemia. *Leuk Lymphoma*. 2022;1–4. doi:10.1080/10428194.2022.2092853